CrystEngComm

Accepted Manuscript

ROYAL SOCIETY OF CHEMISTRY

www.rsc.org/crystengcomm

CrystEngComm

RSCPublishing

ARTICLE

Crystal structures and physicochemical properties of diltiazem base, acetylsalicylate, nicotinate and L-malate

Cite this: DOI: 10.1039/x0xx00000x

D. Stepanovs[a,b], M. Jure[b], M. Gosteva,[a] J. Popelis,[a] G. Kiselovs[a] and A. Mishnev[a,b*]

Received 00th March 2015,
Accepted 00th March 2015

DOI: 10.1039/x0xx00000x
www.rsc.org/

Diltiazem is a drug used as a calcium channel blocker in the treatment of cardiovascular disorders. Because of poor aqueous solubility of the drug, hydrochloride salt has been marketed. Due to the short elimination half-life of diltiazem, extended-release formulations were developed. In the present work, the crystal engineering approach has been employed to obtain diltiazem forms with lower water solubility by treating with carboxylic acids. Three molecular salts of diltiazem with aspirin, niacin and L-malic acid were synthesized and characterized by a single crystal and powder XRD, DTA, solid state CP-MAS, NMR and UV/vis techniques. The single crystal structure determination allowed us to study supramolecular structures and proton transfer interactions from carboxylic acids to diltiazem in the solid state, while NMR studies – interaction in solution. In crystal, the *N*,*N*-(dimethyl)ethylamine fragment of the drug molecule interacts with carboxylic groups of the acids to form heterosynthons. The maximum 40-fold decrease of aqueous solubility is achieved for diltiazem acetylsalicylate hydrate in comparison with the solubility of diltiazem hydrochloride.

Introduction

The cocrystallization approach has recently found an application in the preparation of multicomponent pharmaceutical crystals (MCPC) with improved physicochemical properties.[1–6] These crystals may appear in the form of, *e.g.*, molecular salt or cocrystal; however, the term cocrystal is currently not well-defined.[7] Both molecular salts and cocrystals in pharmaceutical development are aimed primarily to improve solubility and stability[8] or to develop multi-drug solids containing two or more APIs in the same crystal lattice.[3,9]

Both solubility and stability are closely related to the thermal behaviour of the solid. Strong correlations between the melting points of multicomponent pharmaceutical crystals and coformers/counter ions (having similar or homological structures) have been reported in the literature.[2,10,11] Disclosure of such correlations would provide simple rules for rational choice of coformers in the design of MCPC with desirable thermal properties. Solubility being an important property can affect the dissolution rate and, consequently, bioavailability.[1,2]

The present study describes the design, preparation and physicochemical properties of diltiazem pharmaceutical molecular salts with selected carboxylic acids (**Scheme 1**). Salt formation is known to be the first-choice method to improve physicochemical properties of the drug.[12,13] Diltiazem (IUPAC name: [(2*S*,3*S*)-5-[2-(dimethylamino)ethyl]-2-(4-methoxyphenyl)-4-oxo-2,3-dihydro-1,5-benzothiazepin-3-yl] acetate) is a benzothiazepine calcium antagonist and has been marketed for the treatment of cardiovascular disorders.[14] Diltiazem was originally developed as hydrochloride salt and is a Class I drug according to the Biopharmaceutics Classification System (BCS). It has high solubility and high permeability.[15] Preparation of the malate molecular salt has been reported,[16] but, to the best of our knowledge, its X-ray single crystal structure has not yet been reported.

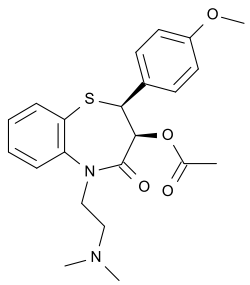

diltiazem (**dil**)

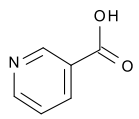

niacin (**nia**)

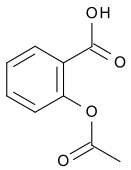

aspirin (**asa**)

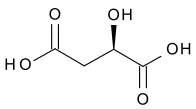

L-malic acid (**mal**)

Scheme 1 The structures and abbreviations of compounds used in this study.

The diltiazem base is very slightly soluble[17], therefore it is used in the form of diltiazem hydrochloride, which is freely soluble in water. Diltiazem is commercially available in the form of immediate-release 30 mg film-coated tablets, administered three or four times daily, and 120-240 mg extended-release capsules administered once daily. Extended-release formulations compensate for the short elimination half-life of diltiazem (3.2±1.3h)[18] and high solubility of diltiazem hydrochloride, which is 565 mg/mL.[19] There have been other reported attempts to develop sustained-release tablets of diltiazem hydrochloride by using polyethylene oxide/polyethylene glycol polymeric matrices[20] or modified guar gum matrix.[21] All mentioned facts

imply that crystal forms of diltiazem with lower solubility would be preferable to include in the formulation. In the present work, we employ the crystal engineering approach[22–26] for the preparation of crystalline diltiazem molecular salts to elucidate how far the cocrystallization approach is able to tailor the solubility of diltiazem. Future work will include investigation of dissolution behaviour, which is related to oral bioavailability.

Results

The diltiazem base (**dil**) was obtained from diltiazem hydrochloride (**dil**-HCl) and used in molecular salts synthesis, namely, diltiazem acetylsalycilate hydrate (1:1:1), or **dil-asa**; diltiazem nicotinate, or **dil-nia** and diltiazem L-malate, or **dil-mal** (Scheme 2 shows the general formula of molecular salts). The method reported herein allowed preparing and characterizing the diltiazem base as a crystalline substance; this was confirmed by both powder and single crystal X-ray diffraction. The formation of molecular salts in the solid state has been proved by powder and single crystal X-ray diffraction, while in-solution formation was observed by nuclear magnetic resonance (NMR).

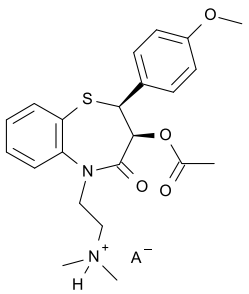

Scheme 2 The chemical structure of diltiazem salt, where A^- represents the organic anion, but the diltiazem is protonated at nitrogen of the tertiary amine.

A decision was made about whether products were cocrystals or salts depending on the values of C–O and C=O bond lengths in the carboxylic groups of the acids in the crystal structures. The ΔpK_a [$\Delta pK_a = pK_{a(base)} - pK_{a(acid)}$] values ranged from 5.33 to 6.74, implying the formation of salt.[27] All the carboxylic groups are deprotonated, as can be inferred from the similar C-O distances (1.233(4) to 1.282(4) Å). Furthermore, in all the molecular structures, hydrogen atoms positions were located from the difference electron density map, showing the transference of hydrogen atoms from an acid to tertiary amino group of a **dil**. So, these considerations unambiguously confirmed that all multicomponent solids were molecular salts.

Strong shifts of *N*-methyl group signals in all molecular salts to the weaker fields, as seen in solid state CP-MAS spectra, are a clear sign of protonation of the amine. Shifts of *N*-methyl group signals correlate with $N_{amine}\cdots O_{acid}$ lengths. The bigger is the distance between N_{amine} and O_{acid} atoms, the more deshielded is the value of N_{amine} chemical shift. N_{amide} signals, in contrary, are positioned more to the stronger fields. Shifts from original positions are not so strong, because here we don't have any direct changes for N_{amide} atoms (spectra is given in ESI, Fig. 1S–2S).

The formation of the salts in solvent was also confirmed by nuclear magnetic resonance. NMR ^{1}H spectra of **dil-asa**, **dil-nia** and **dil-mal** show the changes in chemical shifts in respect to those on the pure **dil** spectrum. Signals of *N*-methyl groups are significantly shielded (chemical shifts are given in ESI S3).

The powder X-ray diffraction (PXRD) patterns of the new compounds are depicted in Fig. 1 in comparison to the PXRD patterns of the initial compounds. The powder patterns of the products show no reflections from initial compounds, indicating complete reactions.

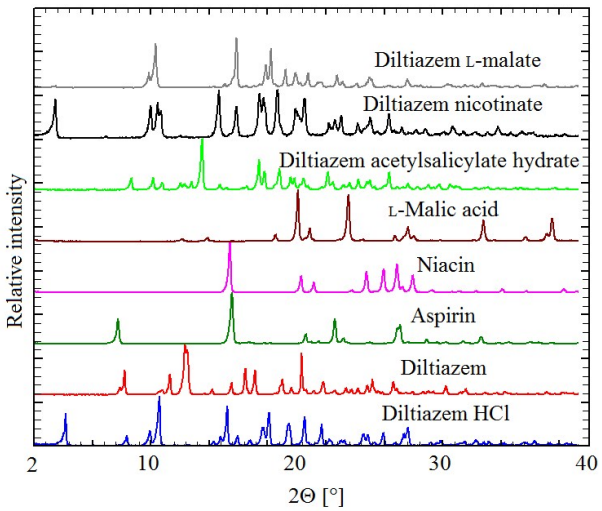

Fig. 1 The experimental PXRD patterns for initial compounds and products obtained after recrystallization.

The calculated[28] X-ray diffraction patterns of **dil**, **dil-asa**, **dil-nia** and **dil-mal** solids and experimental patterns collected for samples after slow solvent evaporation are equivalent (ESI, Fig. 4S–7S), indicating the formation of pure salts. ORTEP-3[29] drawings of the asymmetric units of the structures with atom labelling schemes are given in ESI (Fig. 8S–11S).

Crystal and molecular structure

In all crystal structures the seven-membered ring adopts a twisted boat conformation. The values of the torsion angles in the heterocycle are listed in ESI, Table S12. Methoxy group are almost co-planar with average plane of adjacent phenyl ring. The most flexible fragment in the diltiazem cation is the *N*,*N*-(dimethyl)ethylamine group. The C4–N1–C19–C20 torsion angle characterizing the group's orientation with respect to a heterocycle assumes different values: -101.4(4) for **dil**, -68.7(5) for **dil-asa**, 107.4(3) for **dil-nia** and 107.9(6) for **dil-mal**. Crystal packing of **dil** structure (asymmetric unit is shown in Fig. 2) is stabilized exclusively by van der Waals interactions.

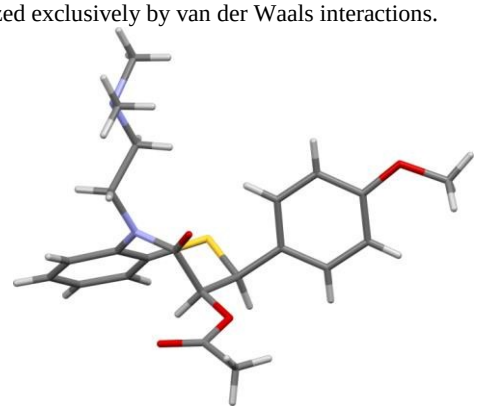

Fig. 2 The asymetric unit of the **dil** crystal structure.

All three salt crystal structures exhibit formation of N–H···O–type hydrogen bonds, and two of them also O–H···O–type bonds (Table 1).

Table 1 Hydrogen bond geometry

D–H···A	D–H (Å)	H···A (Å)	D···A (Å)	∠ D–H···A (°)
		dil-asa		
N2–H2A···O6^{i}	0.89(5)	1.74(5)	2.604(5)	161(4)
O9–H9A···O3^{ii}	0.96(6)	2.20(6)	3.113(5)	160(5)
O9–H9B···O5	0.84(6)	1.97(6)	2.802(5)	174(6)
		dil-nia		
N2–H2A···O5^{iii}	1.05(4)	1.52(4)	2.562(4)	169(4)
		dil-mal		
N2–H2A···O6	0.910(4)	1.889(3)	2.744(5)	155.7(3)
N2–H2A···O7	0.910(4)	2.206(4)	2.820(5)	124.2(3)
O7–H7A···O5^{iv}	0.82	1.93	2.751(5)	177
O9–H9···O7	0.82	2.52	3.008(5)	119.6

(i) 2 – *x*, ½ + *y*, ½ – *z*, (ii) 1 + *x*, -1 + *y*, +*z*, (iii) *x*, -1 + *y*, +*z*, (iv) -1 + *x*, *y*, *z*

In the structure **dil-asa** (Fig. 3 a) supramolecular heterosynthon is made by association of diltiazem cation and acetylsalicylic acid anion *via* N–H···O type hydrogen bond, acetylsalicylic acid anion with water molecule *via* O–H···O type hydrogen bond and water molecule with another diltiazem cation *via* O–H···O type hydrogen bond forming a right-handed helix like chain with graph-set $C_3^3(16)$ [30] along unit cell ***b*** axis (Fig. 4). In **dil-nia** (Fig. 3 b) structure by means of strong hydrogen bond of O–H···O type organic ions are assembled in supramolecular heterodimers with graph-set $D_1^1(3)$ [30]. Analysis of the packing allowed to identify the presence of the homomolecular layers in the crystal structure of **dil-nia**. Thick layers contain bulky diltiazem molecular cations (depicted in red in Fig. 5 a.) while thin layers consist of **nia** anions and are shown in green. The layers are perpendicular to the unit cell ***c*** axis. Within the layers the residues interact by van der Waals forces. The layers are interconnected together by the O–H···O type hydrogen bonds.

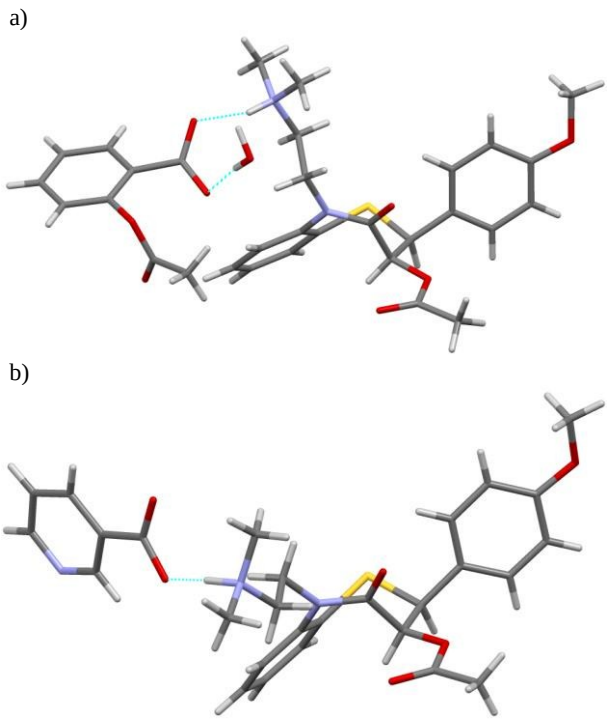

c)

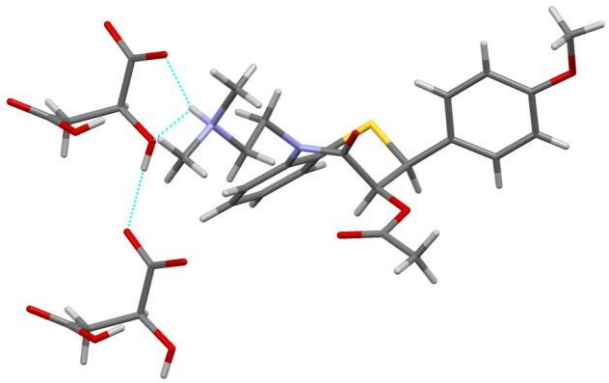

Fig. 3 The fragments of crystal structures of a) **dil-asa**, b) **dil-nia** and c) **dil-mal**. The blue dashed lines indicate hydrogen bonds.

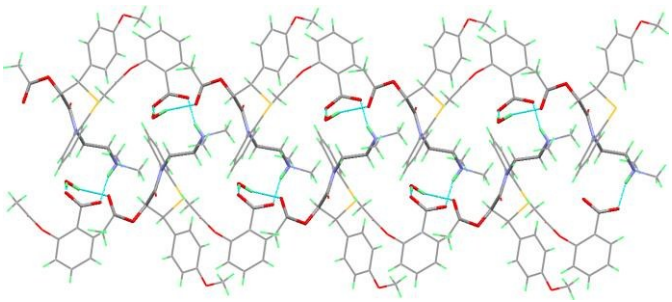

Fig. 4 The fragment of the **dil-asa** crystal structure showing the right-handed helix like hydrogen bonded chain along unit cell ***b*** axis. Atoms participating in the chain are highlighted as capped sticks, while other atoms as wireframes. Hydrogen atoms are shown in light green colour for clarity. The blue dashed lines indicate hydrogen bonds.

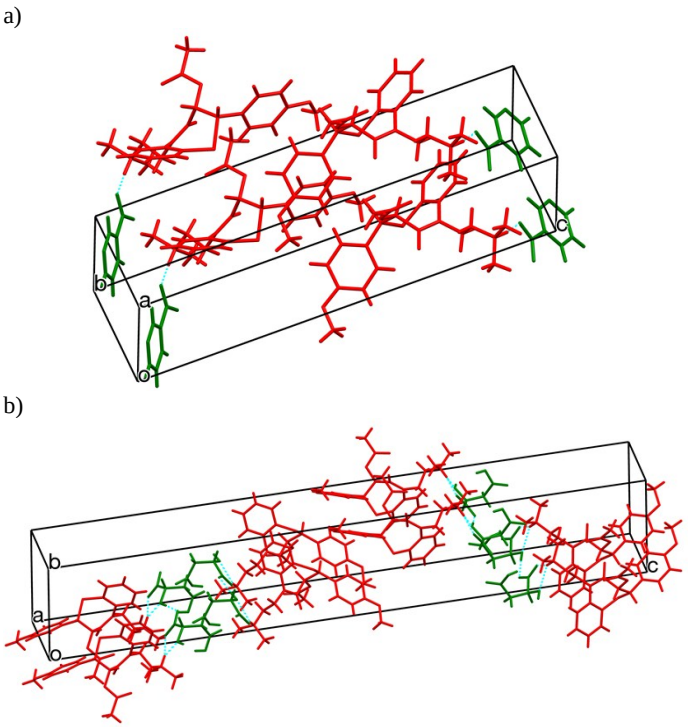

Fig. 5. Crystal structure packing of a) **dil-nia** and b) **dil-mal**. The **dil** cations are shown in red and anions are green. The blue dashed lines indicate hydrogen bonds.

In the structure **dil-mal** (Fig. 3 c) diltiazem cation with L-malate anion forms heterodimers by means of two bifurcated N–H···O type hydrogen bonds with graph-set $R_1^2(5)$. These dimers are further linked *via* O–H···O type hydrogen bonds between L-malate moieties and form chains with graph-set $C_1^1(5)$ [30] along unit cell ***a*** axis (Fig 5 b). The conformation of L-malic acid anions is also stabilized by a week intramolecular hydrogen bond of O–H···O type (Table 1).

Physicochemical properties

It is well-established fact that salts have altered physicochemical properties in comparison with API and salt former. Table 3 summarizes some physicochemical properties of diltiazem and its salts. As follows from the table, the melting point of **dil-asa** is lower than those of API and salt former. This may be attributed to the presence of water molecules in the crystal structure, which are not connected by strong hydrogen bonds to the rest of the structure. The melting point of **dil-nia** lies between melting points of API and salt former, but the melting point of **dil-mal** is higher than those of API and salt former. This may be explained by the formation of extensive two-dimensional networks perpendicular to the unit cell ***c*** axis. The melting point of a crystalline solid depends on a number of factors, including types of intermolecular interactions, symmetry and flexibility of the moieties, as well as arrangement of the moieties in the lattice.[2] Therefore, the discovery of correlations between melting points and other physicochemical properties is not straightforward. Melting points are measured using the DTA method; thermograms are available in the ESI (Fig. S13–S17).

Table 2 Physicochemical properties of **dil** and **dil** salts

Salt	ΔpK_a	Melting point (°C)			Water solubility, mg/ml			
		dil	*acid (salt former)*	*salt*	**dil**	*acid (salt former)*	*salt*	**dil***
dil-HCl	-	105-107	-	212-214	0.48 ± 0.02	-	565[19]	519
dil-asa	5.46		134-136	86-89		4.6	19.0 ± 0.3	12.8 ± 0.2
dil-nia	6.74		236-237	109-112		18	35.4 ± 1.1	27.3 ± 0.9
dil-mal	5.33		128.5-129.5	152-155		558	73.3 ± 1.4	55.4 ± 1.0

*Concentration of **dil** in salt solution

As it was already mentioned, the **dil** as hydrochloride salt is freely soluble, but **dil** base is insoluble in water. According to measured values (Table 2), molecular salts obtained in this work exhibit much higher water solubility than pure API and lower than that of **dil**-HCl. In this work we have varied the solubility, employing a crystal engineering approach. Molecular salts exhibit a 27- to 116-fold increase in the aqueous solubility of diltiazem compared to diltiazem base and a 9- to 40-fold decrease compared with highly soluble diltiazem hydrochloride. This promising result makes a good basis for further development of extended-release formulations of diltiazem.

Experimental

Materials

All chemicals and solvents were obtained from various commercial suppliers and were used as received.

Preparation of diltiazem base

Diltiazem base was prepared from hydrochloride salt. One gram of diltiazem hydrochloride was dissolved in 50 ml of distilled water, and saturated Na_2CO_3 aqueous solution was added up to pH 7.5. Diltiazem base was precipitated out and then extracted using diethyl ether. The extraction process was carried out several times using 50 ml of diethyl ether. Amorphous diltiazem base was obtained after the solvent evaporated. Crystalline substance was obtained after amorphous phase recrystallization from diethyl ether at a temperature of -20°C, giving colourless crystals suitable for a single crystal X-ray diffraction experiment. Recrystallization at room temperature results in amorphous substance.

Single crystal growth and slow solvent evaporation

Diltiazem acetylsalicylate hydrate 1:1:1. **dil** (50 mg, 0.12 mmol) and **asa** (21.7 mg, 0.12 mmol) were dissolved in 5 mL of diethyl ether under ambient conditions and left for evaporation of the solvent at -4 °C (freezer). Single crystals were obtained as colourless blocks in three days.
Diltiazem nicotinate 1:1. **dil** (50 mg, 0.12 mmol) and **nia** (14.8 mg, 0.12 mmol) were dissolved in 5 mL of acetonitrile under ambient conditions and left for slow evaporation of the solvent under ambient conditions. Single crystals were obtained as colourless plates in four days.
Diltiazem L-malate 1:1. **dil** (50 mg, 0.12 mmol) and **mal** (16.2 mg, 0.12 mmol) were dissolved in 5 mL of acetonitrile under ambient conditions and left for slow evaporation of the solvent under ambient conditions. Single crystals were obtained as colourless plates in 4 days.
Bulky samples of **dil**, **dil-asa**, **dil-nia** and **dil-mal** were obtained using the same procedure as in single crystal growth and used in further investigations.

Single crystal X-ray diffraction

X-ray diffraction data were collected using a *Nonius Kappa CCD diffractometer* (CuKα radiation, λ = 0.71073 Å), equipped with a low-temperature *Oxford Cryosystems Cryostream Plus* device. Data were collected using *KappaCCD* Server Software, cell refined by *SCALEPACK*,[31] data reduction performed by *DENZO*[31] and *SCALEPACK*,[31] structures solved by direct method using *SIR2004*[32] and refined by *SHELXL97*[33] as implemented in the program package *WinGX*.[29] Software used to prepare CIF[34] files was *SHELXL97*.[33]

Table3 Selected crystal data, experimental and refinement parameters for structures **dil**, **dil-asa**, **dil-nia** and **dil-mal**

	dil	**dil-asa**	**dil-nia**	**dil-mal**
Empirical formula	$C_{22}H_{26}N_2O_4S$	$C_{31}H_{36}N_2O_9S$	$C_{28}H_{31}N_3O_6S$	$C_{26}H_{32}N_2O_9S$
Formula wt	414.51	612.68	537.62	548.60
Crystal shape	Plate	Plate	Plate	Plate
Crystal colour	Colourless	Colourless	Colourless	Colourless
Crystal system	Orthorhombic	Orthorhombic	Monoclinic	Orthorhombic
Space group	$P2_12_12_1$	$P\ 2_12_12_1$	$P\ 2_1$	$P\ 2_12_12_1$
a (Å)	9.3387(2)	9.9411(4)	8.7897(2)	5.8962(1)
b (Å)	13.9027(4)	10.7606(3)	6.1726(1)	9.0320(2)
c (Å)	16.5550(5)	28.593(1)	25.1531(7)	50.507(1)
β (°)	-	-	91.526(1)	-
V (Å^3)	2149.39(10)	3058.61(19)	1364.21(5)	2689.75(9)
Z	4	4	2	4
D_{calc} (g cm^{-3})	1.281	1.331	1.309	1.355
T (K)	173 (2)	173 (2)	173 (2)	173 (2)
λ(Mo$_{K\alpha}$) [Å]	0.71073	0.71073	0.71073	0.71073
μ(mm^{-1})	0.181	0.163	0.165	0.176
F(000)	880	825	568	1160
No. unique reflns	6221	1296	7311	5177
No. reflns used	4230	4302	4922	1853
No. parameters	266	405	351	346
GOF on F^2	1.01	1.08	1.05	1.00
$R_1[I > 2\sigma(I)]$	0.064	0.098	0.064	0.064
wR_2	0.113	0.150	0.119	0.124
CCDC no.	1056494	1056495	1056496	1056497

Powder X-ray diffraction

Powder diffraction was used to control the results of slow solvent evaporation experiments. Powder X-ray data were collected at room temperature with 0.02° step and scan speed of 0.5 s/step on a *Rigaku ULTIMA IV* powder diffractometer (CuKα radiation, λ = 1.5418 Å) equipped with parallel beam geometry.

Solid state ^{13}C and ^{15}N CP-MAS

Solid state ^{13}C and ^{15}N CP-MAS spectra were acquired on a 800 MHz Bruker Avance III HD spectrometer equipped with a 3.2-mm $^{13}C/^{15}N$ {^1H} E-free MAS probe. The MAS frequency was 15 kHz and the temperature was regulated to 298 K. The CP from ^1H to ^{13}C was performed using a linear ramp (50-100%) with maximum radio frequency (RF) amplitude of 64 kHz on ^1H and with 80.6 kHz on ^{13}C for a contact time of 2 ms. The CP from ^1H to ^{15}N was performed using a linear ramp (50-100%) with maximum RF amplitude of 56 kHz on ^1H and with 43 kHz on ^{15}N for a contact time of 2 ms. Spinal64 decoupling was applied during acquisition with a ^1H RF of 46.8 kHz and a pulse length of 5 us. The acquisition time was 21 ms. The recycle delay was 5-10 seconds. The ^{13}C spectra were referenced externally relative to adamantane. The chemical shift of adamantane CH_2 resonance relative to TMS was 38.48 ppm. The ^{15}N spectra were referenced externally relative to glycine. The chemical shift of glycine relative to liquid NH_3 was 33.4 ppm.

Nuclear magnetic resonance (NMR)

NMR spectra (^1H, ^{13}C) were recorded on *Varian 400MR* spectrometers. Samples were dissolved in [d_6]-DMSO. Chemical shifts are measured relative to TMS (δ = 0) for ^1H, and ^{13}C shifts were referenced to the residual carbon signal of the solvent. ^1H and ^{13}C chemical shifts assignments were supported by 2D ^1H–^{13}C correlations performed on **dil** and **dil**-HCl.

Differential thermal analysis (DTA)

DTA was performed using *Seiko Exstar6000 TG/DTA6300* (Seiko Instruments INC., Japan) equipment. The samples (4–10 mg) were heated in open aluminium pans at a rate of 10°C/ min in nitrogen (flow of 20.0 mL/min).

Fourier-transform infrared spectroscopy (FT-IR)

FT-IR was performed at room temperature on *Shimadzu Corp. IRPrestige-21* spectrometer (FT-IR spectra available in the ESI, Fig. S18–S21).

Solubility experiments and UV/vis spectrometry

The concentration of salt aqueous solutions was determined by UV/vis using *Camspec M501* UV/vis spectrophotometer. UV/vis absorption spectra in the 200–400 nm range were recorded for all samples. One separate linear calibration curve was plotted for (**dil**). The absorption maxima at wavelength 237 nm was used to calculate the concentrations for all samples.

The salt solubility was determined by dissolving excess cocrystal in 5 mL of deionized water at room temperature (23 ± 1 °C). Suspensions were mixed for 24 h. The concentration of the cocrystal in the solution was determined by UV/vis spectrometry, and composition of the solid phase was analyzed by PXRD. UV/vis measurements were performed in triplicate.

Conclusions

Diltiazem base has been prepared in crystalline form and used in synthesis of molecular salts with aspirin (as hydrate), niacin and L-malic acid. Diltiazem base and its salts have been characterized by single crystal X-ray diffraction. Diltiazem moiety in all structures is characterized by seven-membered ring, which adopts a twisted boat conformation. In all salt crystal structures diltiazem cation is protonated at the nitrogen atom of the *N*,*N*-(dimethyl)ethylamine group; this allows formation of N–H···O–type hydrogen bond with corresponding carboxylic acid. The preliminary characterization of new salts has showed a lower solubility as compared with highly soluble diltiazem hydrochloride. Novel molecular salts exhibit 27–116 fold increase in the aqueous solubility of diltiazem compared to diltiazem base and 9–40 fold decrease if compared to highly soluble diltiazem hydrochloride. These promising results make a good basis for further development of formulations of diltiazem with improved bioavailability.

Acknowledgements

We thank Mārtiņš Balodis (University of Latvia) for solid state ^{13}C and ^{15}N CP-MAS analysis. D.S. thanks EC seventh Framework Programme project REGPOT-CT-2013-316149-InnovaBalt for financial support and ERASMUS+ mobility project (No. 2014-1-LV01-KA103-000092) for the opportunity to attend traineeship at CRS4.

Notes and references

[a] Latvian Institute of Organic Synthesis, 21 Aizkraukles street, Riga, LV-1006, Latvia.

[b] Faculty of Materials Science and Applied Chemistry, Riga Technical University, 3 Paula Valdena Street, Riga, LV-1007, Latvia.

Electronic Supplementary Information (ESI) available: [Solid state ^{13}C and ^{15}N CP-MAS, NMR chemical shifts, PXRD

patterns, ORTEP drawings, selected torsion angles, DTA, FT-IR]. See DOI: 10.1039/b000000x/

References

1 E. Batisai, A. Ayamine, O. E. Y. Kilinkissa and N. B. Báthori, *CrystEngComm*, 2014, **16**, 9992–9998.
2 N. Schultheiss and A. Newman, *Cryst. Growth Des.*, 2009, **9**, 2950–2967.
3 M. Žegarac, E. Lekšić, P. Šket, J. Plavec, M. Devčić Bogdanović, D.-K. Bučar, M. Dumić and E. Meštrović, *CrystEngComm*, 2014, **16**, 32.
4 S. Aitipamula, A. B. H. Wong, P. S. Chow and R. B. H. Tan, *Cryst. Growth Des.*, 2014, **14**, 2542–2556.
5 A. Y. Sheikh, S. A. Rahim, R. B. Hammond and K. J. Roberts, *CrystEngComm*, 2009, **11**, 501.
6 C. B. Aakeröy, N. R. Champness and C. Janiak, *CrystEngComm*, 2010, **12**, 22.
7 C. B. Aakeröy and D. J. Salmon, *CrystEngComm*, 2005, **7**, 439.
8 D. J. Good and N. Rodríguez-Hornedo, *Cryst. Growth Des.*, 2009, **9**, 2252–2264.
9 D. Stepanovs, M. Jure and A. Mishnev, *Mendeleev Commun.*, 2015, **25**, 49–50.
10 M. K. Stanton and A. Bak, *Cryst. Growth Des.*, 2008, **8**, 3856–3862.
11 C. B. Aakeröy, I. Hussain and J. Desper, *Cryst. Growth Des.*, 2006, **6**, 474–480.
12 S. M. Berge, L. D. Bighley and D. C. Monkhouse, *J. Pharm. Sci.*, 1977, **66**, 1–19.
13 R. J. Bastin, M. J. Bowker and B. J. Slater, *Org. Process Res. Dev.*, 2000, **4**, 427–435.
14 J. S. Choi and H. K. Han, *Pharmacol. Res.*, 2005, **52**, 386–391.
15 G. Amidon, H. Lennernäs, V. Shah and J. Crison, *Pharm. Res.*, 1995, **12**, 413–420.
16 C. R. Lee, M. Hubert, C. N. Van Dau, D. Peter and A. M. Krstulovic, *Analyst*, 2000, **125**, 1255–1259.
17 T. Takagi, C. Ramachandran, M. Bermejo, S. Yamashita, L. X. Yu and G. L. Amidon, *Mol. Pharm.*, 2006, **3**, 631–643.
18 P. Hermann, S. D. Rodger, G. Remones, J. P. Thenot, D. R. London and P. L. Morselli, *Eur. J. Clin. Pharmacol.*, 1983, **24**, 349–352.
19 X. Han, L. Wang, Y. Sun, X. Liu, W. Liu, Y. Du, L. Li and J. Sun, *Asian J. Pharm. Sci.*, 2013, **8**, 244–251.
20 H. Kojima, K. Yoshihara, T. Sawada, H. Kondo and K. Sako, *Eur. J. Pharm. Biopharm.*, 2008, **70**, 556–562.
21 U. S. Toti and T. M. Aminabhavi, *J. Control. Release*, 2004, **95**, 567–577.
22 C. B. Aakeröy, *Acta Crystallogr. Sect. B Struct. Sci.*, 1997, **53**, 569–586.
23 G. R. Desiraju, *J. Chem. Sci.*, 2010, **122**, 667–675.
24 G. R. Desiraju, *Angew. Chemie Int. Ed. English*, 1995, **34**, 2311–2327.
25 D. Stepanovs, M. Jure, A. Yanichev, S. Belyakov and A. Mishnev, *CrystEngComm*, 2015, **17**, 9023–9028.
26 D. Stepanovs, M. Jure, L. N. Kuleshova, D. W. M. Hofmann and A. Mishnev, *Cryst. Growth Des.*, 2015, **15**, 3652–3660.
27 N. Qiao, M. Li, W. Schlindwein, N. Malek, A. Davies and G. Trappitt, *Int. J. Pharm.*, 2011, **419**, 1–11.
28 C. F. Macrae, I. J. Bruno, J. A. Chisholm, P. R. Edgington, P. McCabe, E. Pidcock, L. Rodriguez-Monge, R. Taylor, J. van de Streek and P. A. Wood, *J. Appl. Crystallogr.*, 2008, **41**, 466–470.
29 L. J. Farrugia, *J. Appl. Crystallogr.*, 2012, **45**, 849–854.
30 J. Bernstein, R. E. Davis, L. Shimoni and N. Chang, *Angew. Chemie Int. Ed. English*, 1995, **34**, 1555–1573.
31 Z. Otwinowski and W. Minor, *Methods Enzymol.*, 1997, 276, 307–326.
32 M. C. Burla, R. Caliandro, M. Camalli, B. Carrozzini, G. L. Cascarano, L. De Caro, C. Giacovazzo, G. Polidori and R. Spagna, *J. Appl. Crystallogr.*, 2005, **38**, 381–388.
33 G. M. Sheldrick, *Acta Crystallogr. A.*, 2008, **64**, 112–22.
34 I. D. Brown and B. McMahon, *Acta Crystallogr. Sect. B Struct. Sci.*, 2002, **58**, 317–324.

Crystal structures and physicochemical properties of diltiazem base, acetylsalicylate, nicotinate and L-malate

D. Stepanovs[a,b], M. Jure[b], M. Gosteva,[a] J. Popelis,[a] G. Kiselovs [a] and A. Mishnev[a,b*]

[a] Latvian Institute of Organic Synthesis, 21 Aizkraukles street, Riga, LV-1006, Latvia.
[b] Faculty of Materials Science and Applied Chemistry, Riga Technical University, 3 Paula Valdena Street, Riga, LV-1007, Latvia.

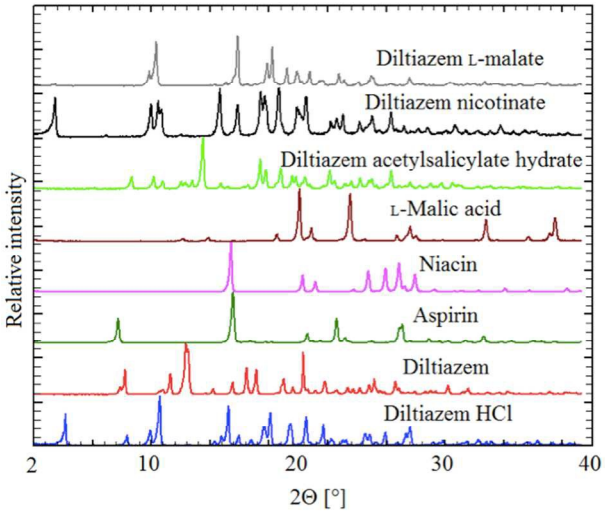

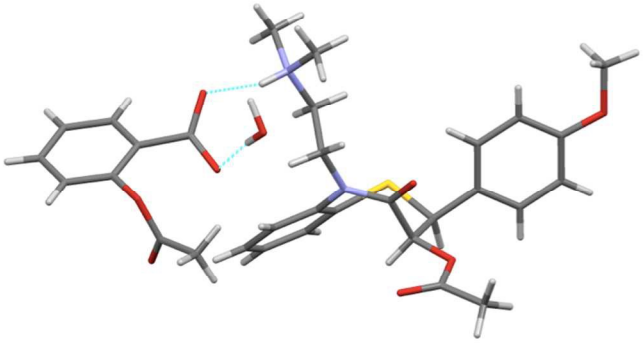

Molecular salts of diltiazem with aspirin, niacin and L-malic acid have been synthesized. Their crystal structures and physicochemical properties have been investigated